한국항행학회논문지
Journal of Advanced Navigation Technology

기반 기술

J. Adv. Navig. Technol. 27(1): 63-70 Feb. 2023

선박 회전축의 무선 센서 시스템의 전원 공급을 위한 회전식 정전용량-무선 전력 전송 시스템

A Rotary Capacitive-Wireless Power Transfer System for Power Supply of a Wireless Sensor System on Marine Rotating Shaft

호앙 반 아이 · 이 영 철*
목포해양대학교 해양전자-통신-컴퓨터공학과

Van Ai Hoang and Young Chul Lee*
Department of Marine Electronic, Communication and Computer Engineering, Mokpo National Maritime University, Jeollanam-do 58628, Korea

[요 약]

본 연구는 선박 추진 축계의 무선 센서 시스템(WSS) 응용을 위한 용량성 무선 전력 전송(C-WPT) 시스템을 제시한다. 커플링 커패시터 양쪽의 단일 Q 팩터 및 회로에서 무효 전력 제거를 위해 양면 LCLC 컨버터 및 변압기 토폴로지가 샤프트에서 WSS용 회전식 C-WPT 시스템을 구동하도록 설계되었습니다. 170pF의 용량을 갖는 병렬 연결된 평행판 회전 커패시터가 설회전축의 C-WPT 시스템용으로 설계 및 구현된다. 실험 결과 C-WPT 시스템은 3mm 거리 및 1 MHz 작동 주파수에서 7.8 W 출력 전력으로 66.67 %의 전송 효율을 달성했다. 따라서 제작된 C-WPT 시스템은 회전축의 WSS에 전원을 공급할 수 있음을 증명하였다.

[Abstract]

In this work, a capacitive wireless power transfer (C-WPT) system is presented for wireless sensor system (WSS) applications in marine propulsion shafts. For a single Q factor on both sides of the coupling capacitor and reactive power removal from the circuit, a double-sided LCLC converter and transformers topology are designed to drive the rotary C-WPT system for WSS on the shaft. Parallel-connected parallel plate rotating capacitors with a capacitance of 170 pF are designed and implemented for the C-WPT system on a snow rotating shaft. In the experimental results, the C-WPT system achieved a transmission efficiency of 66.67% with 7.8 W output power at 3 mm distance and 1 MHz operating frequency. Therefore, it was proved that the fabricated C-WPT system can supply power to the WSS of the rotating shaft.

Key word : Rotating capacitors, Rotating shaft, Transformer, Wireless sensor system, Wireless power transfer.

색인어 : 회전 커패시터, 회전 축계, 변환기, 무선센서시스템, 무선전력전송

http://dx.doi.org/10.12673/jant.2023.27.1.63

Received 1 February 2023; **Revised** 3 February 2023
Accepted (Publication) 17 February 2023 (28 February 2023)

***Corresponding Author; Young Chul Lee**

Tel: +82-61-240-7266
E-mail: leeyc@mmu.ac.kr

Ⅰ. Introduction

Wireless power transfer (WPT) technology has enjoyed increasing popularity in recent year that through the transmission of contactless energy. The WPT is being broadly used and explored for many fields of industrial applications such as charging batteries in mobile devices and electric vehicles, powering biomedical devices and robots, wireless slip rings in rotating machines and much more [1]. So far WPT technology generally can be classified into two types which are inductive WPT (I-WPT) and capacitive WPT (C-WPT). Each type of WPT can be applied according to suitability and requirement of the application. I-WPT uses the principle of the magnetic coupler and is most suitable for low, high-power capability and relatively long distance [2], whereas C-WPT utilizes the principle of the electric coupler and is suitable for low power density and low efficiency [3].

One of the key smart ship technologies for the maritime industry applications, the Internet of Things (IoT) connects devices via the Internet to realize the information sharing, intelligent control, remote monitoring, and data statistics, etc., which significantly improve the intelligence, flexibility, and shipping efficiency, time management, higher output, convenience for our industrial production and daily life [4]. Along with more and more movable electric-driving devices to join the IoT as well as wireless sensor system (WSS), the energy supply is an increasingly serious technique issue for WSS applications. Some rotating mechanisms, either for space, ground or airborne systems, require to transfer the electric power and data while performing a continuous rotation. The use of batteries as a substitute for power cords is not an optimal solution because batteries have a short lifetime, thereby increasing the cost, weight, and ecological footprint of the hardware implementation. Their recharging or replacement is impractical and incurs operating and maintenance costs. At present, the slip ring is widely used in power transfer to the rotating shaft due to its small size, simple structure, and high efficiency. However, the problems of the slip ring bring disadvantages such as wear high maintainability, frictional rotation, physical connection problems and accumulation of the conductive particles [5]. Therefore, in order to overcome the above problems, noncontact technologies have been studied by more and more researchers such as wireless power transfer, energy harvesting and power beaming. Then the usability of WSSs would be significantly improved. In the above technologies, the WPT can be a solution.

An I-WPT system with a rotary transformer allows contactless power transfer to rotary parts to replace the slip ring [6]. However, the problems of inexact connection, radiation, heating of nearby metal, the design of these transformers have reduced power. C-WPT is an emerging solution to wirelessly transfer power based on electric field coupling in the propulsion shaft and has the ability to pass through any metal shielding environment. In recent C-WPT studies, the systems have mainly focused on compensation topologies to increase the power level [7]. To overcome the limitation of compensation networks, a double-sided LCLC compensation topology has been proposed that the system power is proportional to the coupling coefficient, and can be regulated through circuit parameter design without effecting the coupling coefficient [8]. Therefore, it is possible to maintain a high coupling capacitance and the size of the resonant inductor can be significantly reduced. In fact, double-sided LCLC compensation has been used in both I-WPT and C-WPT systems [9]. A double-sided LCLC compensated C-WPT system to transfer a 2.4 kW prototype with 90.8% efficiency for electric vehicles charging through an air gap distance of 150mm [10]. For low power C-WPT systems, it has been utilized for drone charging and data transfer [11]. Although these studies have produced many interesting results with a double-sided LCLC compensation, not much study was done to verify the compensated types of converter topologies used in the field of rotary C-WPT area. In particular, the C-WPT systems only focus on rotary capacitor design. C-WPT can also be applied to a rotary system to avoid power cable connections and achieve 360 degrees rotating freedom [12]. It has been used in the synchronous machine to replace mechanical slip rings [13]. C-WPT systems are much more challenging in implementation. As the coupling capacitance is quite small in the real systems, always in nanofarad (nF) or picofarad (pF) levels, hence the systems require sufficiently high values of quality factor (Q-factor) to realize the designs [14]. It means that C-WPT systems can be extremely sensitive to circuit parameters. The key insight is to insert an extra capacitor in parallel with the coupling capacitor. Therefore, multiple coupling plates are satisfied here to increase the coupling coefficient value.

In this work, the C-WPT system using parallel-connected rotating capacitors has been presented for WSS applications to a propulsion shaft. A double-side LCLC compensated converter was designed, fabricated, and characterized that can get the unity power factor at both sides of the coupling capacitor. In order to decrease the impedance of the coupling capacitance, a step-up transformer is used for this purpose and a step-down transformer reduces the quality factor of the resonant circuit. The optimized Q-factor of the circuit can be obtained by designing turn ratios of the step-up and step-down transformers.

Ⅱ. Design of a C-WPT System

2-1 The design of the WSS system

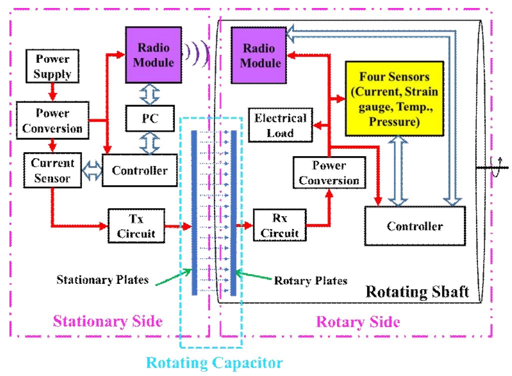

Fig. 1. Block diagram of the WSS with C-WPT system on the rotating shaft.
그림 1. 회전 샤프트에 C-WPT 시스템을 이용한 WSS의 블록도

Fig. 1 shows a block diagram of the WSS with the C-WPT system for monitoring a propulsion shaft. The diagram indicated that the WSS could be provided by the power of the C-WPT system in sensing, collecting, transmitting and receiving data from sensors. The WSS measures transferred power of the C-WPT system, strain, temperature and pressure in the shaft. There are two parts of the WSS, the stationary and rotary sides. The stationary side consists of an electric power conversion, a current sensor, a controller, a transmitter (Tx) circuit, stationary plates and a receiver (Rx) module (XBEE Rx). An electric power conversion converts DC power supply into proper DC level for sensors, controllers, radio modules. A current sensor of the stationary side is used to measure the input power of the C-WPT system. Arduinos are central processing microprocessors of both sides serving with the processing of signals from sensors. The Tx circuit converts DC power to excite stationary plates, which can generate the electric fields and transmit them to the rotary side. The sensing data of the stationary side was sent to the PC via a USB connection and radio module. The rotary side serves two main functions which are sensing, collecting the status condition of the shaft and sending data to an external PC. The wireless sensing modules of the rotary side include four sensors, a controller, and a Tx (radio) module (XBEE Tx) that all should be located on a rotating shaft.

Four sensors include a current sensor, a strain gauge, a temperature sensor and a pressure sensor which are installed in propulsion shaft. The current sensor of the rotate side is used to measure transferred power while in operation. A controller is connected to the sensors and the transmitter for managing power transmission and for monitoring the status of the rotating shaft. The stationary plates convert electric fields back into power through Rx circuit. All obtained data were sent through wireless from the Tx module (XBEE Tx) to XBEE Rx and shown on the PC.

2-2 Double-sided LCLC-compensated converter and transformers for the C-WPT system

The C-WPT uses an electric field and displacement current to transmit wireless power. The DC voltage is converted to AC voltage that provides two stationary metal plates with a high frequency. Then these voltages can be converted to the AC voltage using a rectifier at the output of the load. The small coupling capacitance value is the key challenge in the C-WPT system. Therefore, the best way is to increase the capacitance with an extra capacitor in parallel. The double-side LCLC compensated converter can get the unity Q-factor at both sides of the coupling capacitor. Therefore, the reactive power can eliminate in the circuit.

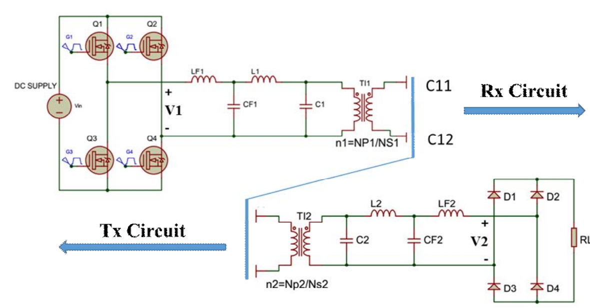

Fig. 2. A double-sided LCLC compensation and transformers circuit of a C-WPT system.
그림 2. C-WPT 시스템의 양면 LCLC 보상 및 변압기 회로.

Table 1. Parameters of double-sided LCLC compensation and transformers circuit.
표 1. 양면 LCLC 보상 및 변압기 회로의 파라미터

Parameter	Value	Unit
V_{cc}	30	V
f	1	Hz
D	50	%
$L_{f1}(L_{f2})$	5.8	uH
$C_{f1}(C_{f2})$	2.2	nF
$C_1(C_2)$	50	pF
$L_1(L_2)$	5.9	uH
$C_{11}(C_{12})$	170	pF
R_L	15	W
$n_1=N_{TI1}$	20/80	T/T
$N_2=N_{TI2}$	50/20	T/T

Fig. 2 shows a design of the double-side LCLC and transformers topology of the C-WPT system on the rotating shaft. The L_{f1}-C_{f1} low pass filter suppresses electromagnetic interference (EMI) noise from the MOSFET-switches bridges. L_{f1}-C_{f1} and L_{f2}-C_{f2} are used on both sides to convert the voltage sources V_1 and V_2 into current sources for the resonant circuits. Capacitance C_{f1} (C_{f2}) can resonate with both inductance L_{f1} and L_1 (L_{f2} and L_2). The other L-C networks (L_1-C_1 and L_2-C_2) are resonated with the equivalent capacitance of the network at the rotary and stationary sides. It is important for the zero-voltage switching of the MOSFET-bridge. Because the coupling capacitance value is small, therefore it is necessary to reduce the impedance value. In order to decrease the impedance of the coupling capacitance, C_{11} and C_{12}. A step-up transformer is used for this purpose and a step-down transformer reduces the quality factor (Q-factor) of the resonant circuit. The optimized Q-factor of the circuit can be obtained by designing turn ratios of the step-up and step-down transformers. In order to simplify the circuit of the system, the fundamental harmonic approximation (FHA) method was used. The LCLC circuit [14] parameters are designed to obtain resonances with the same frequency. The calculated parameters are shown in table 1.

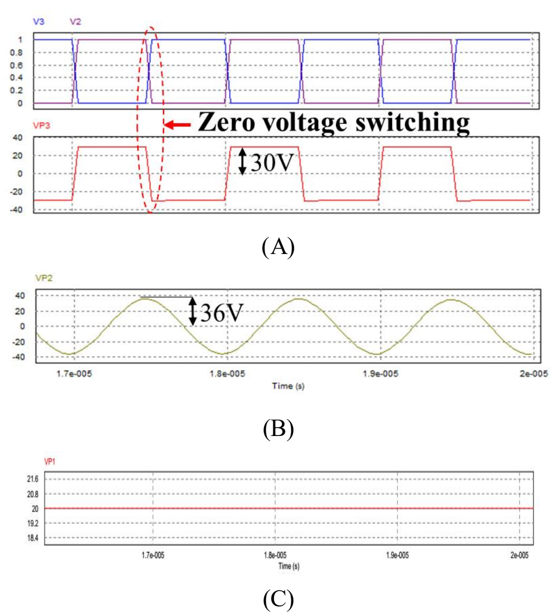

Fig. 3. Simulation results, MOSFET-bridge waveforms (A), Output voltage (VP2) before the rectifier (B), Output voltage (VP1) with a load (C).
그림 3. 시뮬레이션 결과, MOSFET 브리지 파형(A), 정류기 이전의 출력 전압(VP2)(B), 부하가 있는 출력 전압(VP1)(C).

Fig. 3 presents the simulation results of the proposed C-WPT system. The circuit operates at the frequency 1 MHz with a 50% duty cycle. The step-up and step-down transformers have ratios 1:4 and 2.5:1, respectively. In the case of the simulation as shown in Fig. 3 (A), the circuit uses simulation software with specific gating blocks (G) for switches to control the MOSFETs. For the MOSFET-bridge (H-bridge), it consists of four MOSFETs which are simply a set of switches and used to alter the polarity on a circuit thus changing the direction of the voltage and current. In order to control the MOSFET-bridge, two input PWM signals are used to control PWM G_1 (G_4) and G_2 (G_3). The PWM G_1 signal controls Q_1 and Q_4. While PWM G_2 signal controls Q_2 and Q_3. The control signals of the Q_1 and Q_3 are opposite, Q_2 and Q_4 are also opposite. The waveform of the PWM G1 (V_2) and G_2 (V_3) signals are shown in Fig. 3 (A). The output voltage of the MOSFET-bridge VP3 has a symmetrical square waveform and the maximum voltage value from peak to peak V_{p-p} was about 60 V. Fig. 3 (B) indicates that the output voltage before the rectifier of the circuit having the same phase. The peak-to-peak voltage is 36V. After the rectifier, the maximum voltage is 20V as shown in Fig. 3 (C).

2-3 Multiple coupling plate for rotary C-WPT system

Fig. 4 shows the design of the rotating capacitor of the C-WPT system. The capacitive coupling is designed as two series capacitors with equal value, $C_{11} = C_{12}$. In Fig. 4 (B), both C_{11}A and C_{12}B are connected at the stationary side, meanwhile, C_{11}C and C_{12}D are connected at the rotary side. The major target of having multiple-parallel plates is to increase the value of coupling coefficient. It can be convenient to use multiple plates of a smaller capacitance value and size rather than a single one with a larger value and bigger size. In this proposed design, three plates are connected together to form the metal plate C_{11}A and C_{12}B. Similarly, the other two plates are connected together to form metal plate C_{11}C and C_{12}D. The metal plates are connected to form the electrodes of the capacitor. The same dielectric material is applied in between all the plates and placed each other at the distance d. Therefore, in this structure, the four capacitors are formed in one architectural layout as shown in Fig.4 (B). The structure plates of the annulus were used to carry out the capacitive coupling to form the capacitive interface. Fig. 4 (B, C) demonstrates a single round plate of a rotary and stationary plate with an annulus shape to make a rotating capacitor. The total capacitance of the coupling plates and the area of each annulus can be calculated using the annulus formula presented in [1].

Fig. 4 (B) shows a model of capacitive coupling with a three-dimensional structure. A rotating capacitor was designed to install on the shaft as the ruling role of a general capacitor. It helps a rotating capacitor that can operate as a capacitor when the shaft rotates at a high speed without affecting transfer power. Two plates are connected together to form metal rotary plates of an electrode and fixed on the rotating shaft. Similarly, the other three plates are connected in parallel to form metal stationary plates of another electrode and fixed by an external fixture. In this design, aluminum plates are proposed as the annulus plate of the capacitors due to their simplicity, lightness and low cost. Distance between both stationary and rotary plates are separated with d of air gap from 1 to 5 mm. The capacitive coupler for both forward and return directions are equal, $C_{11} = C_{12} = 170$ pF. Thus, C_{11} and C_{12} can be combined into a single capacitor for convenience, that is $C_1 = C_{11}//C_{12} = 170/2 = 85$ pF. There is an available overlapping area that A is equal to 288.1 cm^2. The thickness of all aluminum plates having 2 mm is the same and does not affect the coupling capacitance. In order for the plates to be inserted through the propulsion shaft, a hole with a dimension of 4 cm was punched on each plate. The area of the plate determines the coupling capacitance. The calculated inner and outer radius of the rotary plates, choice 2 cm and 6.85 cm, respectively.

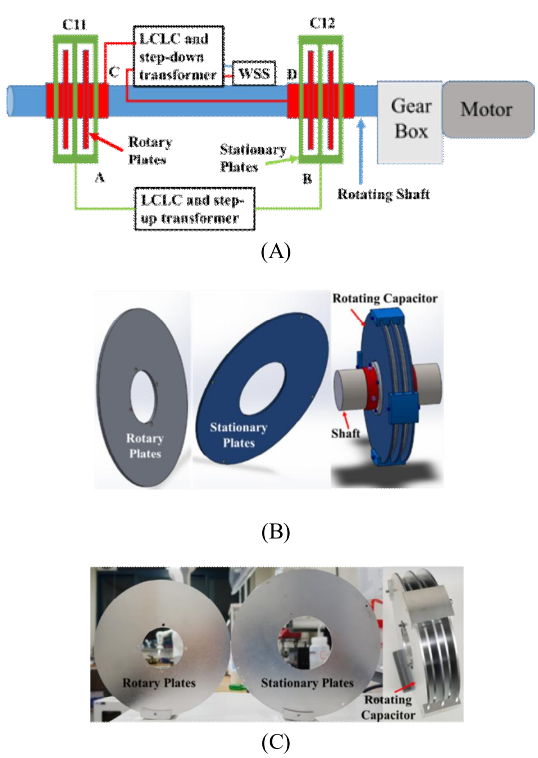

Fig. 4. Rotary capacitor design, Rotating C-WPT framework (A), Designed (B) and Fabricated capacitor(C).
그림 4. 회전 커패시터 설계, 회전 C-WPT 프레임워크(A), 설계(B) 및 제작된 커패시터(C).

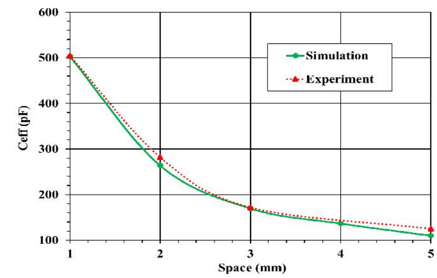

Fig. 5. The capacitance variations with different distance between two plates.
그림 5. 두 판 사이의 거리가 다를 때 커패시턴스 변화.

The assembled capacitor has been shown in Fig. 4 (C). Inner-fixtures hold the rotary plates horizontally and create space between them. These are then attached to the body shaft so that they can be rotated along with the propulsion shaft. The outer-fixtures are attached to the stationary plates and fixed externally, which contributes to keeping the stationary plates fixed in parallel with the rotary disks, and slotting in position at the base frame. The rotary plates are fixed on the shaft and placed at a distance depending on the space between rotary and stationary plates. The stationary plates have an inner radius of 2.7 cm and an outer radius of 7.5 cm. Fig. 5 shows the change of rotating capacitance at the different distances between rotary and stationary plates. It is evident that the capacitance value is inversely proportional to the distance between the rotating plates, meanwhile the distance increases, the capacitance drastically decreases.

Ⅲ. Setup C-WPT System and Measurement Result

3-1 Fabricated C-WPT system

In order to supply power to WSS on the rotating shaft, the C-WPT system which consists of a MOSFET diver, a double-sided LCLC converter, the step-up and step-down transformers, and two rotary capacitors has been installed on the small test shaft as shown in Fig.6. The end-to-end C-WPT system of the experimental setup is carried out with discrete components, on a printed circuit board for the stationary and rotary sides. The front-sided LCLC compensation of the converter and the step-up transformer has been connected to the stationary plates of the two rotating capacitors 1, and 2. The MOSFET driver using PWM (Pulse-width modulation) signals is to control MOSFET-bridge of the converter. The rotary plates have been linked to the step-down transformer, a rear-sided LCLC compensation, a rectifier, and WSS. The WSS includes four sensors (such as DC current sensors, temperature, air pressure and strain gauge), wireless radio modules, and Arduino controllers of the stationary and rotary sides that are also presented in Fig. 6. There is a small rotating shaft connected to the motor via a gear box to simulate the rotational speed by controlling the speed adjustment knob. The radius of the shaft in this work is 2 cm. High speed power MOSFETs (IRF510) were utilized as the inverter switching device. For the full-bridge rectifier circuit at the rotary side, Schottky rectifier diodes (SB3100) were selected to serve as a rectifier. There is extremely low forward voltage, low power loss can be minimized at the rectifier side. Function Generator (DFG-8005 5MHz DDS) was utilized to generate the inverter's PWM signal. It is convenient to fine-tune the duty cycle, D and the switching frequency, f_{sw}.

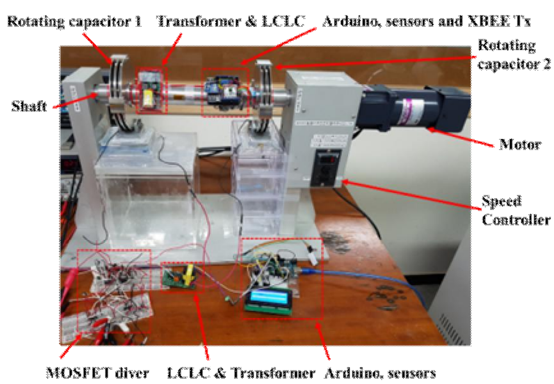

Fig. 6. Experiment setup for WPT system on a small scale test shaft.
그림 6. 소규모 테스트 축계에서 WPT 시스템을 위한 실험 장치.

3-2 Experiment results

The experimental results are shown in Fig. 7 for the rotary C-WPT system on the rotating shaft. Fig. 7 (A) presents the experiment waveform of input voltage across the MOSFET driver. Two switching control signals were used to drive the MOSFET-bridge, which is originally 10 V with frequency 1 MHz at 50 % duty cycle and two gate control signals are different phases in 180 degrees. The zero-voltage switching operation of the full-bridge MOSFET is obtained as shown in Fig. 7 (B). The peak-to-peak output voltage of the MOSFET-bridge is 60 V that the similar to the simulation. This output voltage has been supplied to the front-side LCLC compensation and then a step-up transformer. Output voltage of the step-up transformer has been supplied for two stationary capacitors. At this time point, the process of wireless power transmission was done between rotary and stationary plates. The distance between both plates in this experiment is 3 mm.

The voltage between the two electrodes of the rotary plates is also the input voltage of the primary winding of the step-down transformer TI2. This output voltage is finally rectified via the Schottky diode bridge. The average voltage is about 14.8 V as shown in Fig. 7 (D). The output voltage is relatively stable when the filter capacitor is added before the loading resistor.

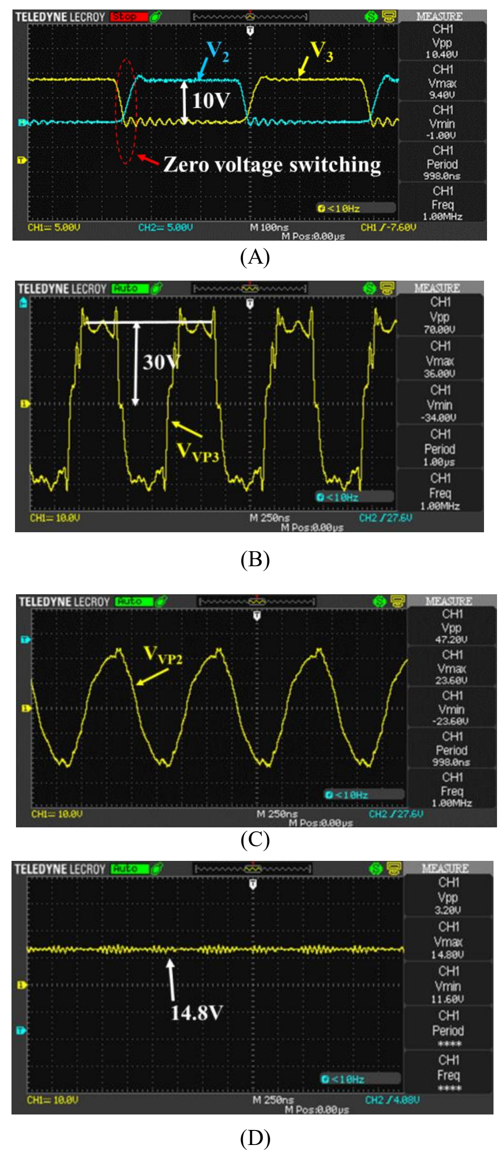

Fig. 7. Experimental results, gate control signal waveforms (A), The output voltage of MOSET-bridge (B), The secondary voltage of the step-down transformer (C), Output voltage after the rectifier (D).
그림 7. 실험 결과, 게이트 제어 신호 파형(A), MOSET-bridge의 출력 전압(B), 강압 변압기의 2차 전압(C), 정류기의 출력 전압(D).

The input power of the double-sided LCLC converter is 11.7 W(30 V×0.39 A). The output power of the C-WPT system is 7.8 W (14.8 V×0.53 A), operated at 1 MHz switching frequency and 30 Ω load. It shows that the C-WPT system can supply 7.8 W output power with 66.67 % efficiency at a 3 mm distance. Fig. 8 shows details about the performance of the system when the load changes, such as it is sufficient power to provide the WSS application to function on the propulsion shaft.

Table 2 shows a comparison of the results obtained with previous works for C-WPTs. As far as we know from previously published literature, our C-WPT presents higher output power compared to the other systems.

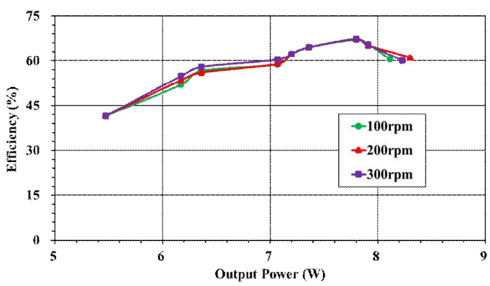

Fig. 8. Efficiency of the C-WPT system.
그림 8. C-WPT 시스템의 효율성.

Table 2. Result comparison of the C-WPTs.
표 2. C-WPT의 결과 비교

Ref.	Structures	Power	Efficiency
[15]	Class-E LCCL for C-WPT	0.97 W	96 %
[16]	Cascaded Boot-Class-E for C-WPT	7.67 W	76 %
[17]	Matrix plate structure	2.5 W	51 %
[18]	Compensation network	1.87 W	85.9 %
[19]	Automatic tuning loops	3.7 W	80 %
This work	A rotary C-WPT System	7.8 W	66.67 %

Ⅳ. Conclusion

In this work, the parallel-plates configuration of the rotating capacitors of the C-WPT system has been presented in detail and described in a rotary form. A practical C-WPT system consisting of the LCLC-compensated converter and transformers topology for supplied power to WSS applications on the propulsion shaft. Initially, the double-sided LCLC-compensated converter and transformers of the circuit were simulated and compared in terms of the output voltage. Then, parallel-connected rotating capacitors (170 pF) are designed and implemented for the C-WPT system on the rotating shaft. A circuit for rotary C-WPT prototype was designed and implemented to demonstrate efficient WPT across the rotating load. It is proven that the power can be transferred to a rotating shaft, in which WSS serves the rotary load. The experimental results have shown that the measured output voltage and power under the rotary coupling configurations are in differed greatly with the theoretical results. The results can obtain 66.67% power transfer efficiency that system being successfully achieved at 1 MHz operating frequency and with 7.8W output power with 3mm distance. This proves the efficiency of the proposed capacitor of the C-WPT system and the validity of the design processes. The C-WPT system could be applied to supply power in the rotating shaft for WSS.

Acknowledgment

This work was supported by Basic Science Research Program through the National Research Foundation of Korea (NRF) funded by the Ministry of Education (2017R1D1A3B03036543).

References

[1] Fei Lu, Hua Zhang and Chris Mi, “A Review on the Recent Development of Capacitive Wireless Power Transfer Technology,” *Energies*, Vol. 10, No. 11, pp. 1752, Nov. 2017.

[2] Lu F., Zhang H., Kan T., Hofmann H., Mei Y., Cai L., and Mi C., “A high efficiency and compact inductive power transfer system compatible with both 3.3 kW and 7.7 kW receivers,” *Proc. of the IEEE Applied Power Electronics Conference and Exposition*, Tampa, FL, USA, pp. 3669–3673, Mar. 2017.

[3] Zhang H., Lu F., Hofmann H., Liu W., and Mi C., “A six-plate capacitive coupler to reduce electric field emission in large air-gap capacitive power transfer,” *IEEE Trans. Power Electron*, Vol. 33, No. 1, pp. 665-675, Jan. 2018.

[4] Hui Yang, S. Kumara, Satish T.S. Bukkapatnam, and Fugee Tsung, “The Internet of Things for Smart Manufacturing: A Review,” *IIE Transactions*, Vol. 51, No. 11, pp. 2472-5862, Jan. 2019.

[5] G. Gao and W. Chen, “Design challenges of wind turbine generators,” *IEEE Electrical Insulation Conference*, Montreal, QC, Canada, pp. 146-152, Jun. 2009.

[6] S. Ditze, A. Endruschat, T. Schriefer, A. Rosskopf, and T. Heckel, “Inductive power transfer system with a rotary

transformer for contactless energy transfer on rotating applications," *2016 IEEE International Symposium on Circuits and Systems*, Montreal, QC, Canada, pp. 1622-1625, Aug. 2016.

[7] Constantin Stancu, Terence Ward, Khwaja M. Rahman, and Robert Dawsey, Peter Savagian, "Separately Excited Synchronous Motor With Rotary Transformer for Hybrid Vehicle Application," *IEEE Transactions on Industry Applications*, Vol. 54, No. 1, pp. 223 – 232, Jan.-Feb. 2018.

[8] Y.-G. Su, Y.-M. Zhao, A. P. Hu, Z.-H. Wang, C.-S. Tang, and Y. Sun, "An Ftype compensated capacitive power transfer system allowing for sudden change of pickup," *IEEE J. Emerg. Sel. Topics Power Electron.*, Vol. 7, No. 2, pp. 1084–1093, Jun. 2019.

[9] F. Lu, H. Zhang, H. Hofmann, and C. Mi, "A double-Sided LCLCcompensated capacitive power transfer system for electric vehicle charging," *IEEE Trans. Power Electron.*, Vol. 30, No. 11, pp. 6011–6014, Nov. 2015.

[10] T. Samanchuen, K. Jirasereeamornkul, C. Ekkaravarodome, "A Review of Wireless Power Transfer for Electric Vehicles: Technologies and Standards," *2019 4th Technology Innovation Management and Engineering Science International Conference*, Bangkok, Thailand, Dec. 2019.

[11] D. Maier, J. Heinrich, M. Böttigheimer, and N. Parspour, "A novel contactless capacitive energy and data transfer system," *Proc. IEEE Wireless Power Transf. Conf*, QC, Canada, pp. 1-4, Jun. 2018.

[12] C. Liu, A. P. Hu, and N.-K. C. Nair, "Coupling study of a rotary capacitive power transfer system," *Proc. IEEE Int. Conf. Ind. Technol.*, pp. 1-6, Feb. 2009.

[13] D. C. Ludois and J. K. Reed, "Brushless mitigation of bearing currents in electric machines via capacitively coupled shunting," *IEEE Trans. Ind. Appl*, Vol. 51, No. 5, pp. 3783–3790, Sep.-Oct. 2015.

[14] Zhenpo Wang, Junjun Deng, Shuo Wang, and Yachao Wang, "A Comparison Study of Compensation Topologies for Capacitive Power Transfer," 2019 IEEE *28th International Symposium on Industrial Electronics (ISIE)*, BC, Canada, Jun. 2019.

[15] Y. Yusop, H. Husin, S. Saat, S. K. Nguang and Z. Ghani, "Class-E LCCL for capacitive power transfer system," 016 IEEE International Conference on Power and Energy (PECon), Melaka, Malaysia, pp. 428-433, 2016.

[16] Yu. Yusmarnita, Saat, Shakir, Abd Ghani, Zamre, Husin, Huzaimah, M.K. Adie, Nguang Sing, "Cascaded Boost-Class-E for rotary capacitive power transfer system," *The Journal of Engineering*, Vol. 2019, 2019.

[17] Liu C., Hu A.P., Dai X, "A contactless power transfer system with capacitively coupled matrix pad," *2011 IEEE Energy Conversion Congress and Exposition, Phoenix, AZ, USA,* pp. 3488–3494, Sep. 2011.

[18] Zhang H., Lu F., Hofmann H., Liu W., Mi C.C, "A Four-Plate Compact Capacitive Coupler Design and LCL-Compensated Topology for Capacitive Power Transfer in Electric Vehicle Charging Application," *IEEE Trans. Power Electron.*, Vol. 31, pp. 8541–8551, 2016.

[19] M. Kline, I. Izyumin, B. Boser, "Capacitive power transfer for contactless charging," *2011 Twenty-Sixth Annual IEEE Applied Power Electronics Conference and Exposition*, TX, USA, pp. 1398-1404, 2011.

호앙 반 아이 (Van Ai Hoang)
2016년 6월 : 베트남해양대학교 해양전자공학과 (공학사)
2020년 3월 : 목포해양대학교 해양전자통신컴퓨터공학과 (공학석사)
※관심분야: wireless power transfer, wireless sensor system and energy harvesting.

이 영 철 (Young Chul Lee)
1995년 2월 : 영남대학교 전자공학과 (공학사)
1997년 8월 : 영남대학교 전자공학과 (공학석사)
2005년 2월 : 한국과학기술원 공학과 (공학박사)
2005년 3월~2017년 2월: 목포해양대학교 해양전자통신공학부 조교수, 부교수
2017년 3월~현재: 목포해양대학교 해양메카트로닉스학부 교수
2018년 1월~현재: 한국 ITU-R SG3 연구위원
2010년 4월~2011년 2월: Telecom Malaysia Research & Development (TMRND) 기술고문
※관심분야: 초고주파 시스템 집적, System-on-Package (SoP), 밀리미터파 시스템 및 회로 설계, 국제표준 전파모델